

A MULTIDISCIPLINARY STUDY OF LATE PLEISTOCENE-HOLOCENE SEDIMENTS OF THE GAETA BAY CONTINENTAL SHELF

F.O. Amore - G. Ciampo - V. Di Donato - P. Esposito - M. Pennetta - E. Russo Ermolli - D. Staiti - A. Valente
Dip.to di Scienze della Terra, Università di Napoli "Federico II", Napoli, Italy

RIASSUNTO - *Studio multidisciplinare su sedimenti del Pleistocene superiore-Olocene della piattaforma continentale del Golfo di Gaeta* - Il Quaternario *Italian Journal of Quaternary Sciences*, 9(2), 1996, 521-532 - Vengono qui presentati i risultati dello studio di due carotaggi a gravità (G93-C5 e G93-C8) realizzati nel Golfo di Gaeta, a circa 20 km dalla foce del Fiume Garigliano, in sedimenti del tardo Pleistocene e dell'Olocene. Sono state studiate attraverso l'analisi quantitativa le associazioni a foraminiferi, nannofossili calcarei, ostracodi e pollini. Per la carota G93-C8 sono ancora in corso le analisi polliniche e dei nannofossili calcarei. I sedimenti sono stati caratterizzati mediante analisi geotecniche e granulometriche che hanno consentito di distinguere diverse unità deposizionali. Nelle due carote è distinguibile una unità inferiore con sedimenti fangosi tipici di una fase di *highstand*. La parte basale delle due carote è caratterizzata da associazioni a foraminiferi planctonici tipiche di acque fredde. Tra le associazioni a nannofossili calcarei si riscontrano alte percentuali di *Coccolithus pelagicus*, anch'esso indicatore di acque fredde. Gli spettri pollinici mostrano alte percentuali di *taxa* erbacei, fra cui gli elementi steppici (*Artemisia*), indicatori di clima freddo, raggiungono picchi del 20%. I *taxa* arborei sono dominati dal *Pinus*. Le ostracofaune sono dominate da specie prevalentemente infralitorali che indicano profondità non superiori ai 30-40 m. Le unità sabbiose sono caratterizzate da consistenti percentuali di foraminiferi bentonici costieri (*Ammonia* spp., *Elphidium* spp.) e le ostracofaune sono dominate da specie tipiche di substrati sabbiosi che indicano una batimetria non superiore ai 20 m. Quest'intervallo rappresenta un ambiente di spiaggia sommersa riferibile verosimilmente alla base della trasgressione tardiglaciale-olocenica. A partire da questi livelli e fino al *top* delle carote l'incremento nelle associazioni a foraminiferi planctonici e a nannofossili calcarei di specie tipiche di acque tropicali e sub-tropicali ma anche l'abbondanza di *Quercus* deciduo e di Xerofite mediterranee (in particolare *Quercus* tipo *ilex*) indicano un progressivo incremento delle paleotemperature. Il corrispondente aumento della batimetria viene evidenziato dall'aumento percentuale di ostracodi ad *habitat* prevalentemente circalitorale. Sulla base delle associazioni a foraminiferi planctonici, a nannofossili calcarei e dall'analisi pollinica (in particolare i picchi massimi di *Quercus* e *Quercus ilex*) l'*optimum* climatico olocenico può essere posizionato tra 90 e 130 cm nella carota G93-C5 e intorno ai 30 cm nella carota G93-C8. Le variazioni delle associazioni a foraminiferi planctonici sono state utilizzate per porre dei vincoli cronologici nell'intervallo olocenico delle carote.

ABSTRACT - *A multidisciplinary study of Late Pleistocene-Holocene sediments of the Gaeta Bay continental shelf* - Il Quaternario *Italian Journal of Quaternary Sciences*, 9(2), 1996, 521-532 - A multidisciplinary study was carried out on two cores (G93-C5 and G93-C8) from the Gaeta Bay continental shelf to characterize the sediments. Different depositional units have been distinguished on the basis of sedimentological and geotechnical analyses. These units have characters indicative of deposition in shallow to relatively deep environments. Paleoecological analyses were based on foraminifera, ostracoda, calcareous nannofossils and pollen assemblages. Both cores consist of a lower silty unit with cold climate fossil assemblages. This unit is overlain by a sandy unit which identifies the beginning of temperature increase trend. The fossil assemblages of this unit, in particular benthic foraminifera and ostracoda, are rich in shallow water and sandy bottom species. In both cores the upper unit consists of silty and clayey levels of a late glacial-holocene sedimentary body with warm climate fossil assemblages.

Keywords: Sedimentology, paleoclimatology, Late Pleistocene-Holocene, Tyrrhenian Sea, foraminifera, nannofossils, ostracoda, pollen
Parole chiave: Sedimentologia, paleoclimatologia, Pleistocene superiore-Olocene, Mar Tirreno, foraminiferi, nannofossili, ostracodi, pollini

1. INTRODUCTION

A multidisciplinary study was carried out on two gravity cores (G93-C5 and G93-C8) from the Gaeta Bay continental shelf (Fig. 1). The G93-C5 Core, 500 cm long, was taken at 111 m b.s.l. (41°05'41"N 13°35'56"E). The G93-C8 Core, 362 cm long, was taken at 126 m b.s.l. (41°04'31"N 13°32'18"E). A large number of samples were taken from each core and analysed. In particular, sedimentological studies were carried out by M. Pennetta and A. Valente, foraminifera were studied by V. Di Donato and D. Staiti, calcareous nannofossils and ostracods were determined by O. Amore, P. Esposito and G. Ciampo, respectively and pollen analyses were carried out by E. Russo Ermolli.

2. SEDIMENTOLOGY

Sediment recovery was made with a Kulleberg-type gravity corer. After determining the physical proper-

ties of the sediments (wet- and dry-bulk density $\rho_{(WBD)}$, $\rho_{(DBD)}$; grain density, G_s ; porosity, η ; water content $W_{c(WWC)}$, $W_{c(DWC)}$; and undrained cohesion, C_u), descriptions (lithology, colour, hardness and disturbance degree) and sampling were carried out. The regular 10 cm sampling interval was reduced when lithological variations became frequent. Fifty-four samples were taken from the C5 core (Fig. 2) and 43 from the G93-C8 core (Fig. 3). Calcimetric and granulometric analyses were also performed with the standard sedimentology methods. The obtained data allowed for the classification of the sediments (Shepard, 1954) and the inference of Folk & Ward's (1957) statistical parameters. Finally, a quick microscope analysis on 300 grains, more than 63 μ in diameter, allowed us to determine both the content in clastic and bioclastic grains (complete or fragmentary shells) and their roundness.

The basal part of the recovered succession (from 500 to 245 cm in Core 5 and from 362 to 145 cm in Core 8) consists of dark grey (5Y 4/1) silt and silty-sand (Mz = 5.5-4.3 ϕ : medium to coarse silt). In particular, the most

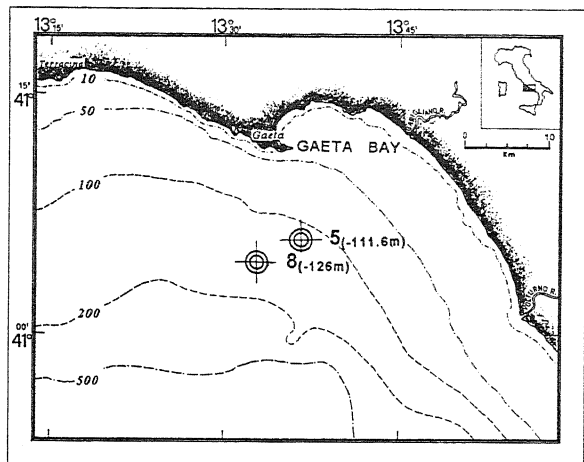


Fig. 1 - Off-shore drilling locations.
Ubicazione delle stazioni di campionatura.

distal sediments (Core 8; Fig. 3) are generally moderately coarser ($Mz: 4.3-4.8\phi$: coarse silt) than those collected in a more proximal position (Core 5; Fig. 2). In the basal unit it is possible to recognize a general coarsening upward trend. At the core bottom the frequency curve skewness tends towards a fine fraction.

Calcium carbonate values remain steady (around 25%). Physical properties (Figs. 2 and 3) indicate a degree of consolidation greater than that of more recent over-lying sediments ($Cu = 0.25 \text{ kg/cm}^2$, on the average). The high values of the dry-bulk density ($\rho_{(DBD)} = 0.25 \text{ kg/cm}^3$) suggest a proximal source area (Chassefiere & Monaco, 1987) and, therefore, shallow water environment.

Only in core 5, a poorly sorted, graded volcanic layer is interbedded from 265 to 285 cm. Here, the frequency curve skewness tends towards a coarse fraction.

An erosional surface separates the basal unit from the intermediate one (Figs. 2 and 3). This mostly consists of olive grey (5Y 4/2), graded, poorly sorted (uni- or bimodal) bioclastic silty sands ($Mz = 4.3-3.6\phi$: very fine sands), in which the curve skewness tends towards a fine fraction. In core 5 these sediments are concentrated only in one level, 65 cm thick (from 245 to 180 cm). In core 8 the same sediments are split into three different layers (from 141 to 131 cm; from 122 to 91 cm and from 91 to 55 cm) separated by two dark grey (5Y 4/1) graded volcanoclastic levels (from 145 to 141 cm; and from 131 to 122 cm) classified as fine sand in which the poor sorting is due to the abundant silty matrix. In G93-C8 core the bioclastic succession is less thick (50 cm) than in C5 core. The calcium carbonate content, 35-38% on the average, reaches values of about 50% at the base of the graded levels. The dry-bulk density varies around $1.2-1.3 \text{ gr/cm}^3$.

The upper part of the succession (Figs. 2 and 3) is 180 cm thick (core 5) and becomes gradually thinner seaward up to 50 cm (core 8). It consists mainly of bioturbate moderately-sorted clayey to sandy silt ($Mz = 4.8-7.1\phi$: fine to very fine silt), with soft firmness, and whose colour gradually passes from olive grey (5Y 4/2) to olive (5Y 4/3). This sediment is characterized by leptocurtic curves, skewed towards the coarse fraction. The level is graded and with plane-parallel lamination at its base.

The saturated sediments are characterized by very low values of both undrained cohesion ($Cu < 0.1 \text{ kg/cm}^2$) and dry-bulk density ($\rho_{(DBD)} = 0.64-1.05 \text{ gr/cm}^3$). Void index and porosity have high values, in agreement with recent and poorly consolidated sediments. Calcium carbonate values remain steady (around 22% in core 8 and 18% in core 5). Sorting of core 5 (mostly moderately sorted) seems higher than in core 8 (mostly poorly sorted). In the intermediate unit of both cores, sorting is poor. Such a poor sorting, especially for the most distal core (C8), may indicate, in a coastal marine environment, a forced deposition or a medium poor sorting capacity in a large sediment contribution environment. This poor sorting capacity is suggested by the positive skewness value frequency recorded in the lower and intermediate units of core 8 and in the intermediate unit of core 5.

In the Mz/Sk_1 (Friedman, 1961) diagram, a faintly negative correlation between the two parameters (Fig. 4) can be seen. The most recent fine sediments, with negative skewness coefficient values, consist of calcium carbonate planktonic tests and terrigenous muds, as reported by Gensous *et al.*, 1993.

Despite the slight increase in the skewness coefficient recorded towards coarser samples, Sk_1 values are mostly negative in the bioclastic sandy samples, identifying almost symmetrical to asymmetrical curves towards the coarse fraction. The coarse samples could be correlated with high energy hydrodynamic processes, which were strong during a sea level lowering phase and still active during the successive sea level rise on the outer shelf and on the upper slope (Marani *et al.*, 1986). Such processes cleaned up the material causing the re-suspension of the finest particles (Valia & Cameron, 1977). The volcanoclastic samples present negative Sk_1 values too. This could be ascribed to the abundant silty matrix, which influences the main mode and to the pyroclastic material low specific weight, which does not constitute the mode.

In the $CaCO_3/\rho_{(DBD)}$ diagram (Fig. 5) it is worth noting that, $CaCO_3$ content being equal, there are sediments with variable $\rho_{(DBD)}$ values. Most recent sediments and bioclastic sands, characterized by low dry-bulk density, were probably deposited in more distal environments than those lying at the bottom (Snoeckx & Rea, 1994).

The dry-bulk density (Figs. 2 and 3) is on the average higher in the deepest sandy-silt level than in the most superficial one ($\rho_{(DBD)} = 1.5 \text{ g/cm}^3$ with respect to an average value of 0.8 g/cm^3). This is linked to the clastic grain abundance (Chassefiere & Monaco, 1987), which is higher in this shelf zone during sea-level lowstands.

Porosity and void index reach the lowest values (50%) because of the compaction of deepest sediments. The whole core Cu values (except for the bioclastic level) are lower in the most superficial sediments (0-150 cm) because of the lack of consolidation. In these sediments Cu is always below 0.1 kg/cm^2 . Cu values slightly increase in the deepest sediments where a higher consolidation degree occurs ($Cu \approx 0.25 \text{ kg/cm}^2$). The different availability of terrigenous sediment also influences the dry-bulk density: $CaCO_3$ contents being equal, the $\rho_{(DBD)}$ is higher when the lithic fraction is higher (Snoeckx & Rea, 1994).

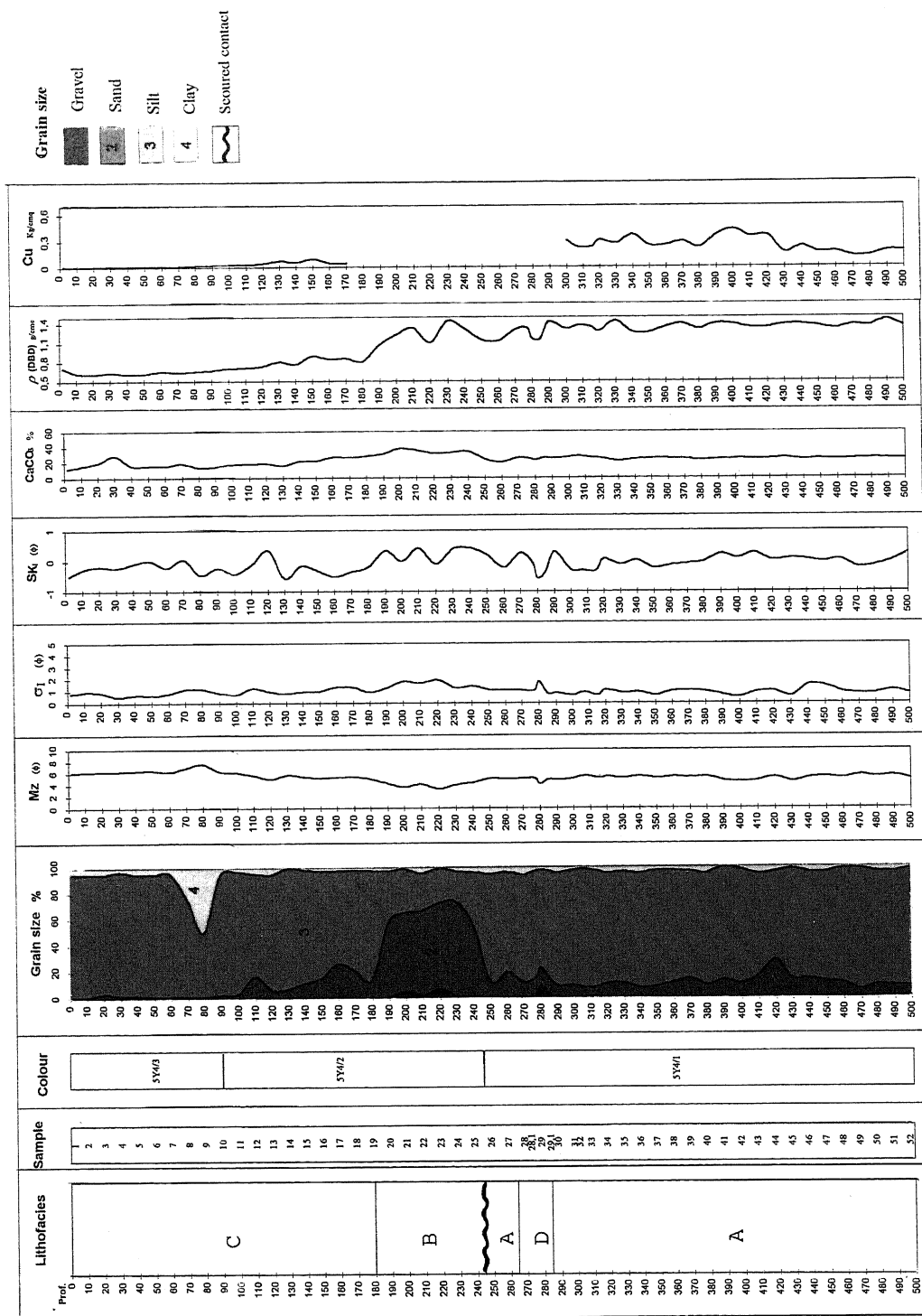


Fig. 2 - G93-C5 Core. Correlation between sedimentological characters and physical properties. Lithological units: A = lower unit; B = intermediate unit; C = upper unit; D = volcanoclastic levels. Units below the erosional contact are Late Pleistocene in age, units above the erosional contact are Late Glacial Holocene in age.
 Carota G93-C5. Correlazione fra le caratteristiche sedimentologiche e le proprietà fisiche. Unità litologiche: A = unità inferiore; B = unità intermedia; C = unità superiore; D = livelli vulcanoclastici. Le unità al di sotto del contatto erosionale sono del Pleistocene superiore; quelle al di sopra sono del Tardi Glaciale-Olocene.

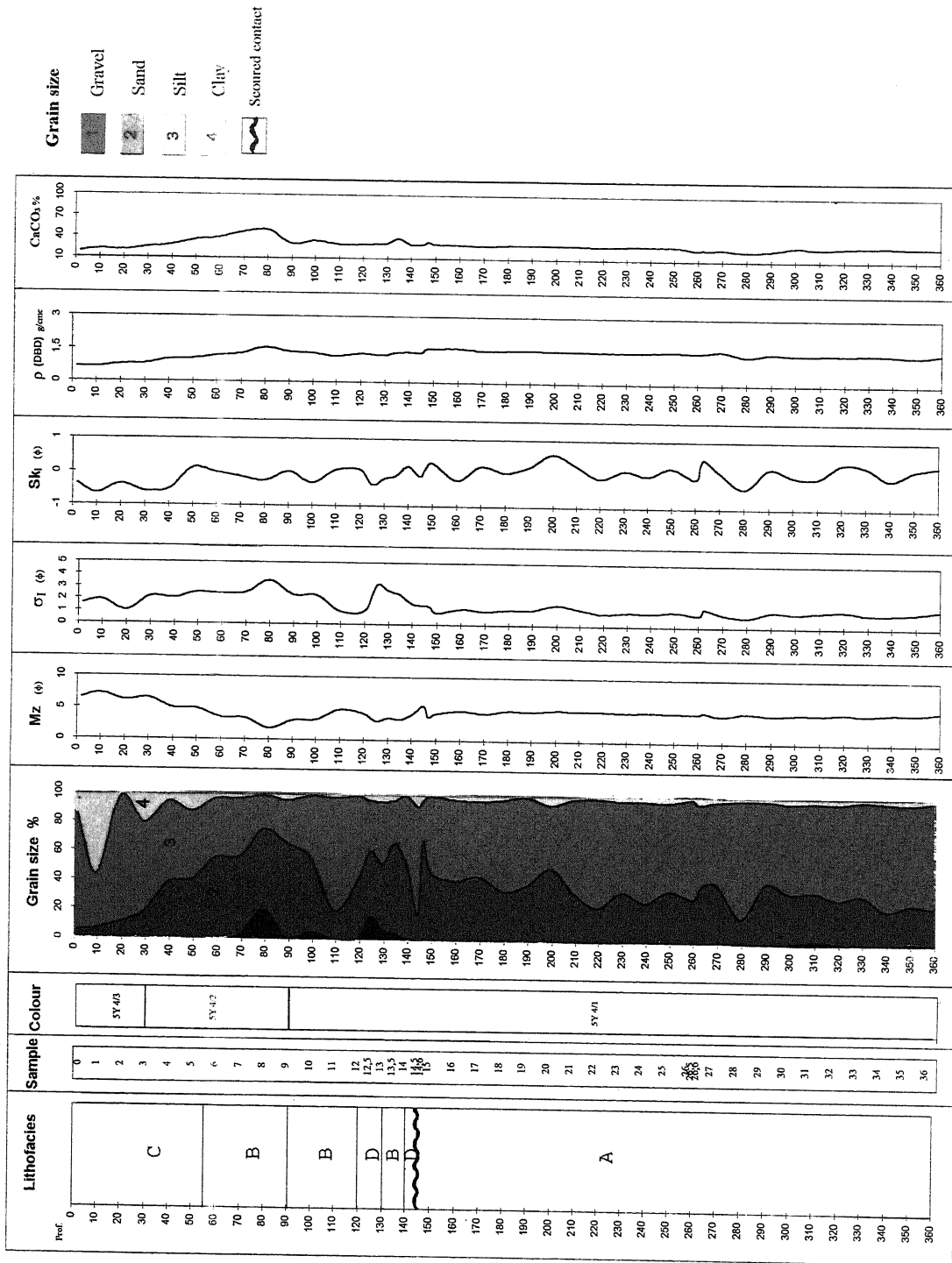


Fig. 3 - G93-C8 Core. Correlation between sedimentological characters and physical properties. Lithological units: A = lower unit; B = intermediate unit; C = upper unit; D = volcanoclastic levels. Units below the erosional contact are Late Pleistocene in age, units above this contact are of the Late Glacial.

Carota G93-C8. Correlazione fra le caratteristiche sedimentologiche e le proprietà fisiche. Unità litologiche: A=unità inferiore; B=unità intermedia; C = unità superiore; D = livelli vulcanoclastici. Le unità al di sotto del contatto erosionale so del Pleistocene superiore, quelle al di sopra di tale contatto sono del Tardi Glaciale.

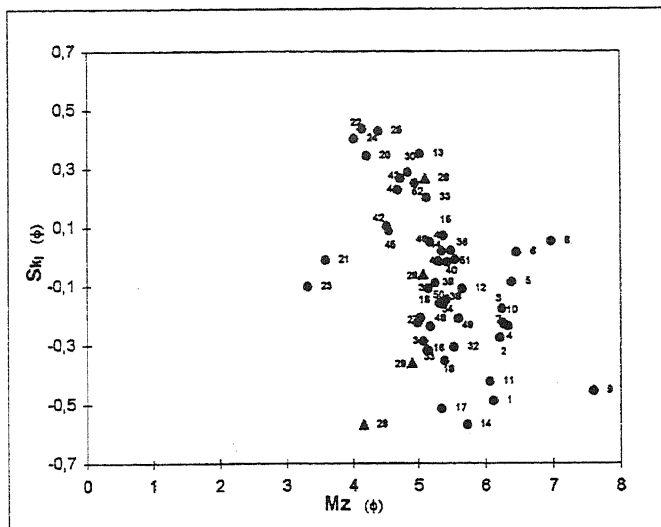


Fig. 4. Core G93-C5. Mean size versus skewness.

Carota G93-C5. Diagramma del granulo medio in rapporto all'asimmetria.

(*Argilloecia acuminata*, *Buntonia textilis*, *Parakrithe dimorpha*, *Polycope* spp.) (Fig. 11c, d).

In the upper part of both cores, there is good agreement with the events pointed out by the fossil associations (Fig. 7 and Fig. 11). In core G93-C5 the sandy unit above the erosional surface representing the base of the transgression, is characterized by fair percentages of near-shore benthic foraminifera (i.e. *Ammonia* spp., *Elphidium* spp.). The ostracod assemblages include typically sandy substratum and/or shallow water species such as *Callistocythere flavidofusca*, *Costa edwardsi*, *Lepto-*

3. PALAEOECOLOGY

In the basal unit of core G93-C5, the planktonic foraminiferal associations are dominated by cold water species (*Globorotalia scitula*, *Neogloboquadrina pachyderma*, *Turborotalita quinqueloba*) the percentage of which fluctuates around 30% (Fig. 6e, f, g and Fig. 7a). *G. inflata* is represented mainly by morphotypes of *Globorotalia oscitans*. The calcareous nanofossil assemblages are characterized by a low diversity which results in the dominance (up to 50-60%) of the cold water species *Coccolithus pelagicus* (Brand, 1994) (Fig. 7c and 8e). In the same interval, the pollen spectra show high percentages of herbaceous taxa (mainly Poaceae, Asteraceae and Chenopodiaceae) (Fig. 9g). Among them steppic elements (*Artemisia*, *Ephedra* and *Hippophae*) reach peaks of about 20% (Fig. 7e and 9h). These spectra are indicative of a landscape dominated by typically cold climate open formations. The arboreal taxa are poorly diversified and dominated by *Pinus* (Fig. 9d), a great pollen producer which statistically dominates the spectra during glacial periods. In the core G93-C8 the dominance of cold water foraminifera in the lower silty unit is also evident (Fig. 10e, f, g).

In the basal part of the core G93-C5, the ostracod assemblages are mainly characterized by infralittoral species (*Cythereis uffendorfei*, *Leptocythere* spp., *Semicytherura* spp.) indicating a maximum depth of 30-40 m (Fig. 7g). Between 325 and 350 cm a slight decrease in the infralittoral species and an equivalent increase in deeper habitat species is observed (*Argilloecia* spp., *Polycope demulderi*, *Henryhowella sarsi*) (Fig. 7f, g). This slight deepening coincides with a relative rise in temperature, as evidenced in the same interval by both the planktonic foraminifera and the pollen assemblages (Fig. 7a, e). Analogous observations can be made in the lower silty unit of core G93-C8. However, in this core a general deeper bathymetry (50-70 m) is shown by lower percentages of benthic foraminifera (*Ammonia* spp. and *Elphidium* spp.) and of infralittoral ostracod species as well as by the constant presence (with low percentages) of deep habitat ostracod species

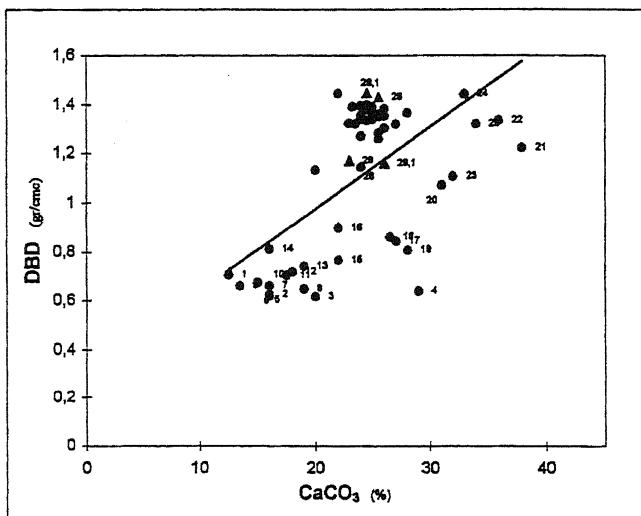


Fig. 5 - Core G93-C5. Calcium carbonate contents versus dry-bulk density.

Carota G93-C5. Diagramma del contenuto in carbonato di calcio in rapporto alla massa di volume secca.

cythere levis, *Loxococoncha rhomboidea*, *Semicytherura incongruens* (Fig. 12c) and others, indicating depths around 20 m. Moreover, benthic associations in this unit show a considerable remoulding (Fig. 11f and Fig. 12b). Among assemblages of calcareous nanofossils the abrupt increase in percentage of *Braarudosphaera bigelowi* (Fig. 8f) recorded in this interval, may be linked to a sudden fresh water arrival (Müller, 1979).

From these levels the increasing percentages of warm water planktonic foraminifera and calcareous nanofossils, as well as the composition of pollen assemblages indicate a progressive paleotemperature increase (Fig. 7). Among foraminifera an increase in *G. ruber*, *Orbulina universa* and tropical species (*Globigerinella digitata*, *Globigerinella siphonifera*, *Globigerinoides trilobus* s.l., *Globoturbotalita rubescens*, *Globoturbotalita tenella*, *Hastigerina pelagica*) is recorded (Fig. 6). In the upper part of the core, scattered specimens of *G. ruber* var.

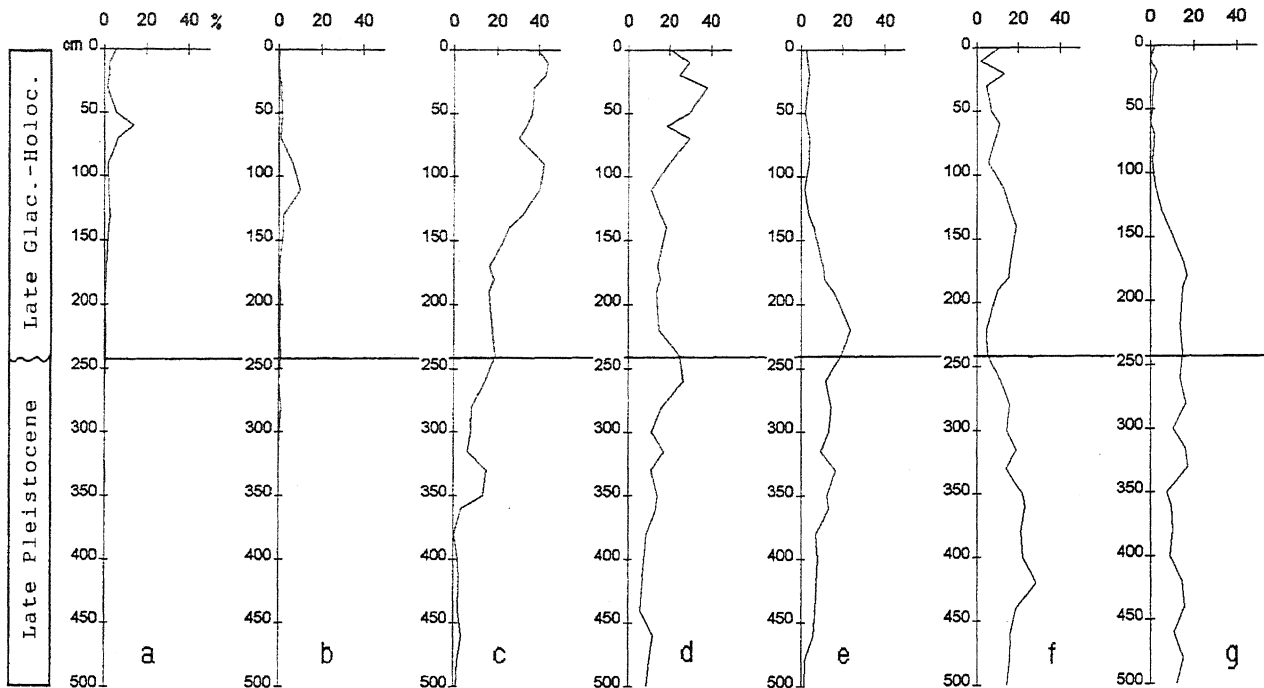


Fig. 6 - Core G93-C5. Percentages of selected planktonic foraminifera. (a): *O. universa*; (b): *G. trilobus s.l.*; (c): *G. ruber*; (d): *G. bulloides*; (e): *G. inflata*; (f): *T. quinqueloba*; (g): *N. pachyderma*.

Carota G93-C5. Percentuali delle specie di foraminiferi planctonici più significative. (a): *O. universa*; (b): *G. trilobus s.l.*; (c): *G. ruber*; (d): *G. bulloides*; (e): *G. inflata*; (f): *T. quinqueloba*; (g): *N. pachyderma*.

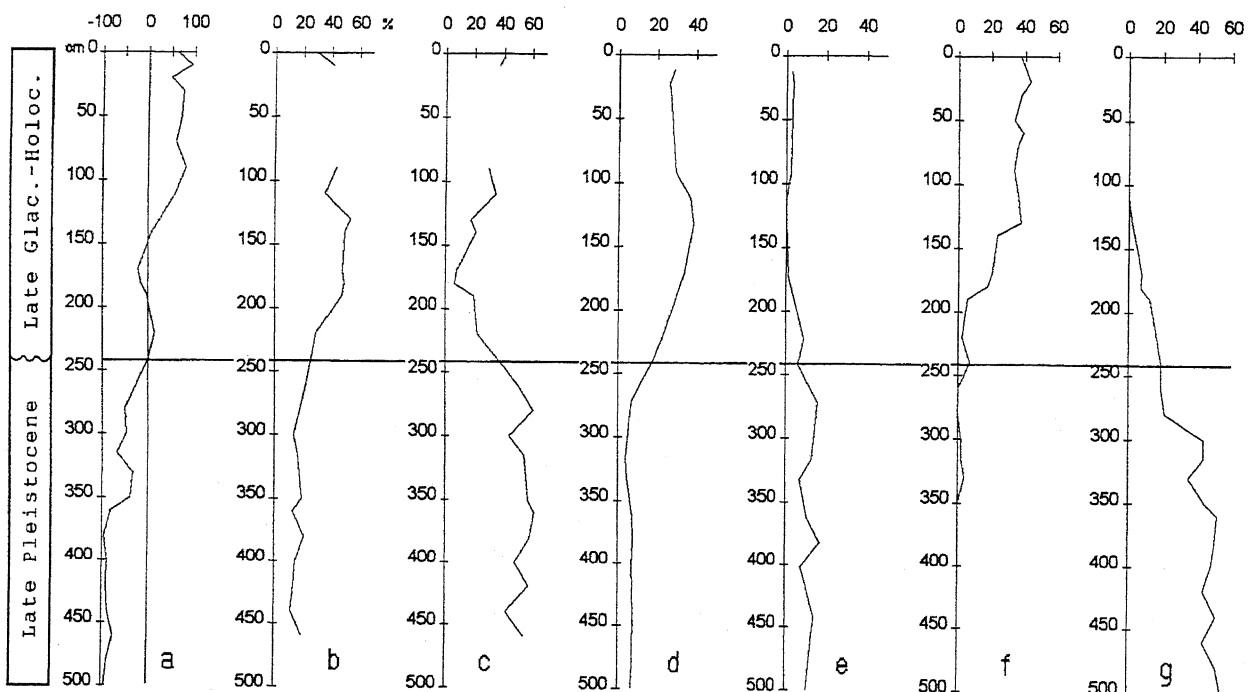


Fig. 7 - Core G93-C5. Comparison between climatic and bathymetric markers. (a): climatic curve based on planktonic foraminiferal assemblages [(Warm-Cold/Warm+Cold) \times 100]. Calcareous nannofossils. (b): percentages of warm water species; (c): percentages of the cold water species *Coccolithus pelagicus*; Percentages of pollen taxa. (d): *Quercus* sp. (e): steppic elements. Ostracods. (f): percentages of off-shore species; (g): percentages of near-shore species.

Carota G93-C5 - Confronto tra markers climatici e batimetrici. (a): curva climatica basata sulle associazioni a foraminiferi planctonici [(Caldi-Freddi/Caldi+Freddi) \times 100]. Nannofossili calcarei. (b): percentuali delle specie calde; (c): percentuali di *Coccolithus pelagicus*, specie fredda. Percentuali dei taxa pollinici. (d): *Quercus* sp. (e): elementi steppici. Ostracodi. (f): percentuali delle specie profonde; (g): percentuali delle specie costiere.

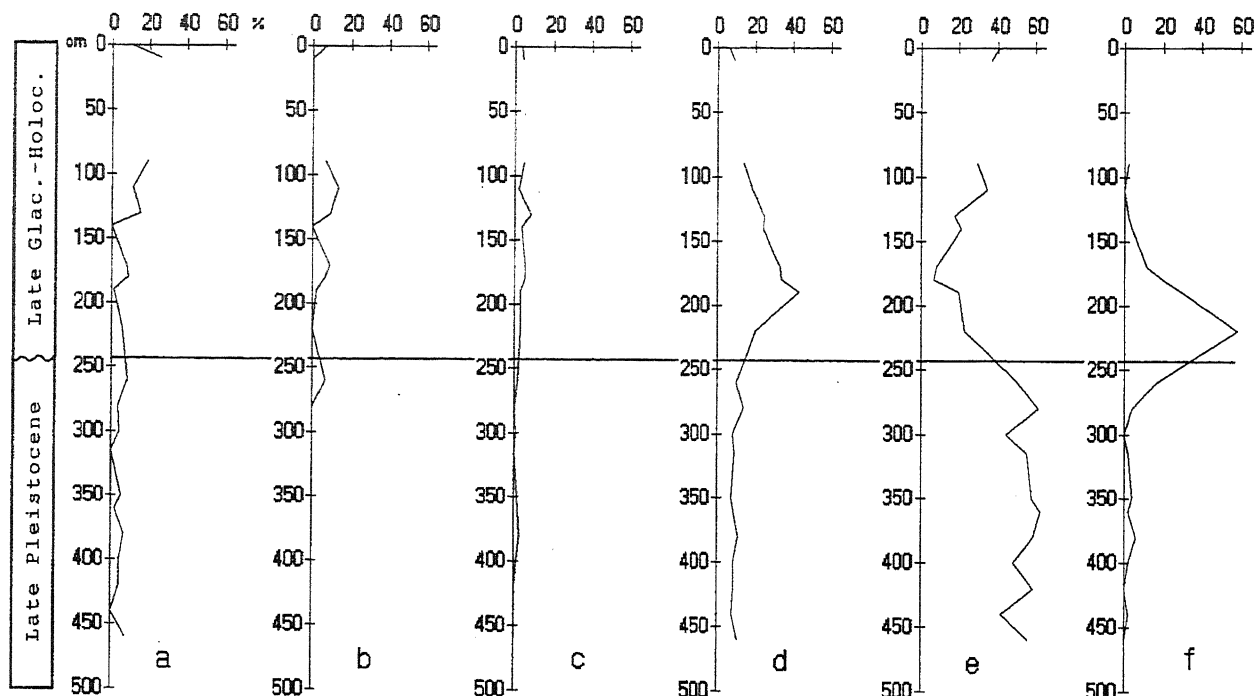


Fig. 8 - Core G93-C5. Percentages of selected calcareous nannofossils species: (a): *Syracosphaera pulchra*; (b): *Ceratolithus* spp.; (c): *Rhabdosphaera clavigera*; (d): *Calcidiscus leptoporus* and *Umbilicosphaera mirabilis*; (e): *Coccolithus pelagicus*; (f): *Braarudosphaera bigelowi* ($\times 10$).

Carota G93-C5. Percentuali delle specie più significative tra i nannofossili calcarei. (a): Syracosphaera pulchra; (b): Ceratolithus spp.; (c): Rhabdosphaera clavigera; (d): Calcidiscus leptoporus e Umbilicosphaera mirabilis; (e): Coccolithus pelagicus; (f): Braarudosphaera bigelowi ($\times 10$).

rosea were also found. The percentages of *Neogloboquadrina pachyderma* "left" – always lower than those of *N. pachyderma* "right" – are strongly reduced in the Holocene interval of core G93-C5 (<2%).

The highly diversified calcareous nannofossil assemblages are characterized by the increase in *Calcidiscus leptoporus*, *Rhabdosphaera clavigera*, *Umbilicosphaera mirabilis*, *Ceratolithus simplex*, *C. telesmus*, *C. cristatus*, and *Syracosphaera pulchra* (Fig. 8). Pollen spectra are increasingly enriched in arboreal taxa, in particular the deciduous oak and the mediterranean xerophytes rapidly increase their percentages to the detriment of the herbaceous taxa (Fig. 9). The pollen spectra of this interval indicate the rapid development of a typically warm and wet climate phase. The increase in the deciduous *Quercus* curve corresponds in this case to the increase in temperature which marks the beginning of the Holocene. Oak pollen is a good terrestrial climate indicator, its increase indicating climate amelioration (Rossignol-Strick & Planchais, 1989). The maximum abundance of warm species in the associations is located between 90 and 130 cm. This event can be interpreted as the Holocene climatic optimum. A bathymetric deepening, corresponding to a temperature increase, is indicated by the sudden increase of circum-littoral ostracod species such as *Argilloecia* spp., *Henryhowella sarsi*, *Polycopse* spp., *Parakrithe dimorpha* etc. (Fig. 7f), and by the contemporaneous decrease of the benthic foraminifera *Ammonia* spp. and *Elphidium* spp.

These events are not so marked in core G93-C8, where they can be recognized between 10 and 30 cm (Fig. 12). As emphasized by the correlation between the two cores, core G93-C8 lacks surface sediments because of the present-day erosion.

4. BIOCHRONOLOGY

Although the low bathymetry of both sites is a restrictive element for the composition of planktonic assemblages because deep water species are less abundant, the quantitative analyses performed for the holocenic interval of core C5 allow for the identification of events which can be correlated with those reported for other areas in the Mediterranean Sea. In this chronostratigraphic unit, analyses of calcareous nannofossil assemblages indicated the *Emiliania huxley* peak, associated with *Gephyrocapsa oceanica* >5 μm (Rio *et al.*, 1990). Among planktonic foraminifera the abrupt percentage increase of *Globigerinoides* gr. *ruber* and the almost contemporary decrease in abundance of subpolar species (*i.e.* *Neogloboquadrina pachyderma*), recorded in core G93-C5 between 130 and 170 cm (Fig. 6c, g), were also observed in sediments from the Alboran Sea (Pujol & Vergnaud Grazzini, 1989) between 9,500 and 10,000 yr B.P., in correspondence with the end of deglaciation. In the North Levantine and Adriatic Sea, these events mark the boundary between Zones I and II (9,600 yr B.P.) which are differentiated

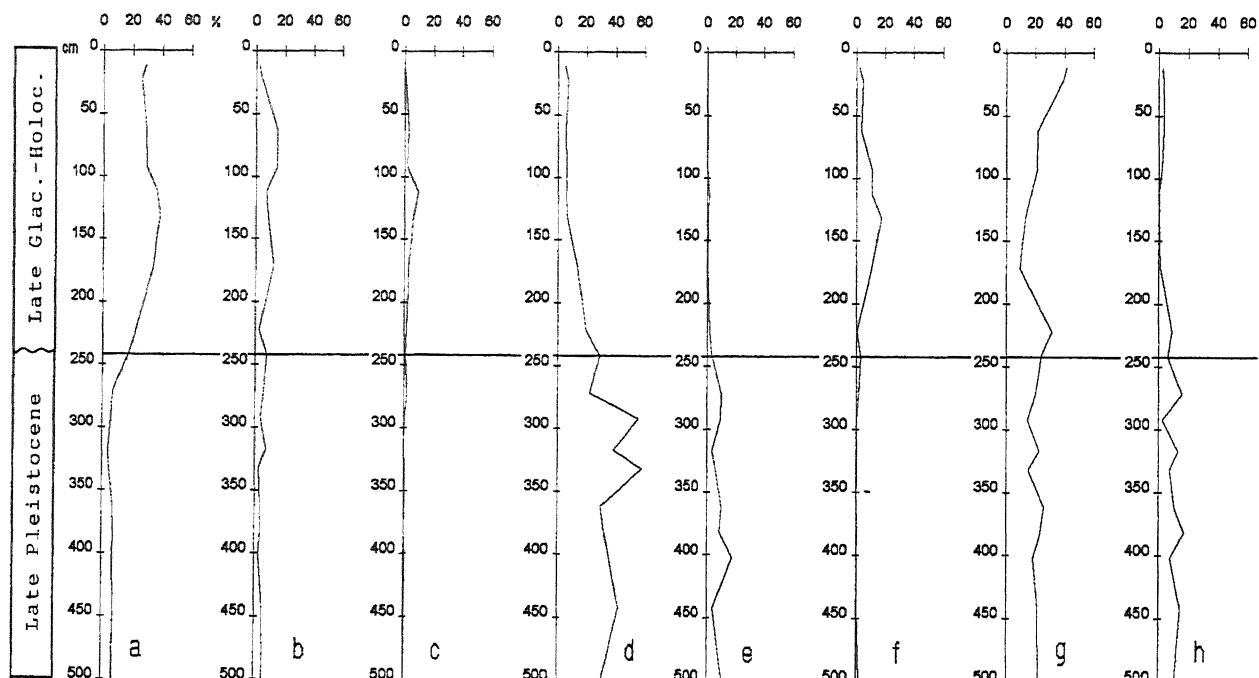


Fig. 9 - Core G93-C5. Simplified pollen diagram. (a): *Quercus* sp.; (b): *Carpinus*, *Alnus*, *Ulmus*, etc.; (c): *Fagus* and *Betula*; (d): *Pinus* and undetermined Pinaceae; (e): *Abies* and *Picea*; (f): mediterranean xerophytes (*Quercus* type *ilex*, *Olea*, *Phillyrea*, etc.); (g): herbaceous elements (Poaceae, Asteraceae, Chenopodiaceae, etc.); (h): steppic elements (*Artemisia*, *Ephedra* and *Hippophæe*).

Carota G93-C5. Diagramma pollinico semplificato. (a): *Quercus* sp.; (b): *Carpinus*, *Alnus*, *Ulmus*, etc.; (c): *Fagus* e *Betula*; (d): *Pinus* e Pinaceae indeterminabili; (e): *Abies* e *Picea*; (f): xerofite mediterranee (*Quercus* tipo *ilex*, *Olea*, *Phillyrea*, etc.); (g): elementi erbacei (Poaceae, Asteraceae, Chenopodiaceae, etc.); (h): elementi steppici (*Artemisia*, *Ephedra* e *Hippophæe*).

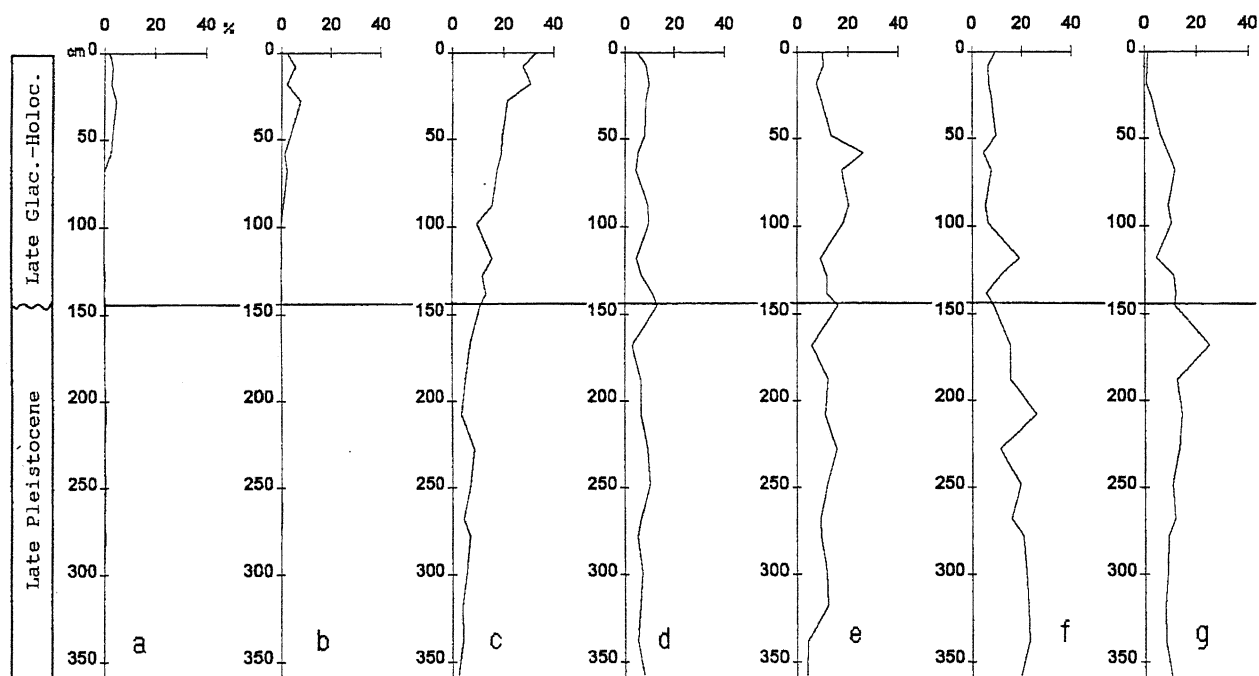


Fig. 10 - Core G93-C8. Percentages of selected planktonic foraminifera. Letter symbols as in Figure 6.

Carota G93-C8. Percentuali delle specie di foraminiferi planctonici più significative. Le lettere corrispondono a quelle della Figura 6.

on the basis of the planktonic foraminifera frequency patterns (Jorissen *et al.*, 1993; Rohling *et al.*, 1993). The peak in the abundance of the deep water species *Globorotalia inflata*, reported in the basal part of Zone I

for both the Adriatic and Tyrrhenian Sea (Jorissen *et al.*, 1993) was not recorded in core G93-C5, probably because of the shallow depositional environment. The small peak in the abundance of *Globigerina bulloides*

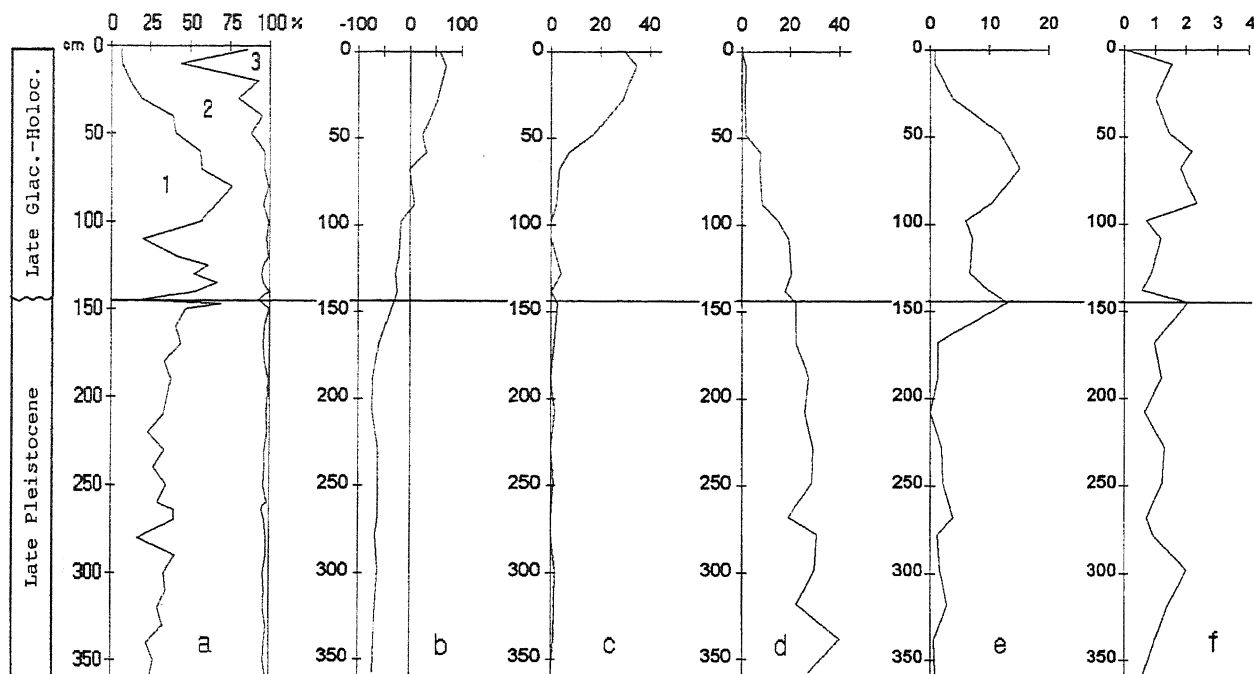


Fig. 11. Core G93-C8. (a): Granulometric log; (b) climatic curve based on planktonic foraminiferal assemblages [(Warm-Cold/Warm+Cold) \times 100]; Ostracods: (c) percent of off-shore species; (d): percent of near-shore species; (e): percent of *Semicytherura incongruens*; (f): reworking index based on the right valves/left valves ratio of selected species.

Carota G93-C8 - (a): Log granulometrico; (b) curva climatica basata sulle associazioni a foraminiferi planctonici [(Caldi-Freddi/Caldi+Freddi) \times 100]; Ostracodi: (c) percentuali delle specie profonde; (d) percentuali delle specie costiere; (e) percentuali di *Semicytherura incongruens*; (f) indice di rimaneggiamento basato sul rapporto valve destre/valve sinistre di specie scelte.

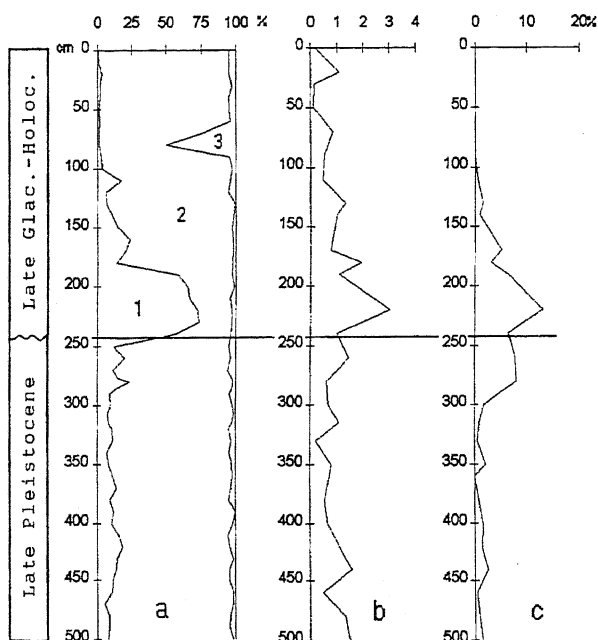


Fig. 12 - Core G93-C5. Comparison of granulometric log (a), reworking index of ostracoda (b) (see Fig.11) and percentages of *Semicytherura incongruens* (c).

Carota G93-C5. Confronto tra il log granulometrico (a), l'indice di rimaneggiamento per gli ostracodi (b) e le percentuali di *Semicytherura incongruens* (vedi Fig. 11).

and the peak of *Turborotalita quinqueloba* recorded at 140 cm (Fig. 6d, f) might correspond to the abrupt increase in *T. quinqueloba* percentages recorded at 9,000 yr BP in the Alboran Sea (Pujol & Vergnaud Grazzini, 1989). This was related to an increase in nutrient availability in surface waters at the end of deglaciation. Between 90 and 110 cm an increment in the *G. trilobus* percentages was observed (Fig. 6b) as well as the maximum abundance of *G. ruber* (Fig. 6c). The estimated ages of the same events are 7,800 yr (Jorissen *et al.*, 1993) and 7,000 yr BP (Pujol & Vergnaud Grazzini, 1989), respectively. The abundance increase of *G. bulloides* in the upper part of core G93-C5 (Fig. 6d) was also reported for different areas of the Mediterranean Sea (Pujol & Vergnaud Grazzini, 1989; Jorissen *et al.*, 1993; Rohling *et al.*, 1993; Capotondi *et al.*, 1996). The contemporary abrupt disappearance of calcareous nannofossils (Fig. 8) and dinoflagellate cysts in the palynological slides may suggest a high productivity in surface water.

In core G93-C8 the post-glacial period is represented by only 145 cm of sediments (Fig. 11), the surface sediment being eroded. Some events recognized in core G93-C5 were also found in G93-C8. The increase in *G. ruber* percentages (Fig. 10c) is more evident between 70 and 30 cm, while *N. pachyderma* percentages (Fig. 10g) are drastically reduced to 0%. The 9,000 yr BP relative abundance peak of *T. quinqueloba* is recorded at 48 cm (Fig. 10f). At 58 cm *G. inflata* reaches its maximum abundance (Fig. 10e). According to Jorissen *et al.* (1993) this event has an estimated age of 9,300 yr. The abundance peak of *G. trilobus s.l.* at 28 cm (Fig. 10b) can be correlated

with that found at about 100 cm in core G93-C5.

The lower units of both cores are devoid of bio-chronological constraints. They can only be ascribed to an ill-defined moment of the last glacial period.

5. CONCLUSIONS

The lower silty unit corresponds to a regressive phase as indicated by the upward coarsening trend, the presence of coarser sediments in the most distal core and by a preliminary analysis of acoustic profiles (Senatore, unpublished data). These identify a prograding wedge system with seaward deeper clinofolds, as observed in other sectors of the Tyrrhenian margin (Correggiari *et al.*, 1992; Pennetta, 1996). In this unit foraminifera, nannofossils and pollen assemblages indicate cold climate conditions. In fact, foraminiferal associations are characterized by high percentages of *Neogloboquadrina pachyderma* and *Turborotalita quinqueloba*. *Coccolithus pelagicus* dominates the nannofossil assemblages and high amounts of herbaceous and steppic elements (*Artemisia*) characterize the pollen assemblages. In the same unit, the predominance of *Cytherois uffenordei* and *Leptocythere ramosa* in ostracod assemblages reveals a shallow water depositional environment. The sediments of the intermediate (bioclastic) and upper (silty and clayey) units represent the late glacial-holocene sedimentary body. Their thickness gradually decreases seaward because of the combined action of sea level rise and sedimentary input from the Garigliano River. Moreover, superficial and deep streams of the Mediterranean and Tyrrhenian Sea can erode large amounts of sediments and thus may represent another controlling factor on the holocene deposit geometry (Got *et al.*, 1985; Trincardi & Normark, 1988). This could explain the small thickness of core G93-C8 upper unit. The rapid increase of arboreal taxa (deciduous *Quercus* particularly), the disappearance of steppic elements and the increase of foraminifera and nannofossils warm water species (*Globigerinoides spp.*, etc.; *Calcidiscus leptoporus*, *Ceratolithus spp.*, etc.) show a temperature increase. The consequent deepening of bathymetry is indicated by the change of ostracods assemblages, which are here characterized by the predominance of *Henryhowella asperima* and *Argilloecia acuminata*. Comparisons based on quantitative analyses of planktonic assemblages with other sites of the Mediterranean Sea, allowed coeval events to be recognized. Such correlations gave some chronological constraints to core stratigraphy. The Holocene climatic optimum was identified between 90 and 130 cm in core 5 and between 10 and 30 cm in core 8.

ACKNOWLEDGEMENTS

This study is part of a research programme directed by Prof. T.S. Pescatore, and dealing with the evolution of continental margins. The main programme is financially supported by the MURST 40% grant.

CITED REFERENCES

- Brand L.E., 1994 - *Physiological ecology of marine coccolithophores*. In: *Coccolithophores* (Winter A. & Siesser W.G., eds.), Cambridge University Press, 39-49.
- Capotondi L., Morigi C., Cespuglio G. & Borsetti A.M., 1996 - *Biostratigraphic and paleoceanographic records during the last deglaciation in the southern Adriatic sea*. In: Evans S.P., Frisia S., Borsato A., Cita M.B., Lanzinger M., Ravazzi C. & Sala B. (a cura di), *Modificazioni climatiche ed ambientali tra il Tardiglaciale e l'Olocene antico in Italia*, Abstracts, Convegno AIQUA - MTSN, Trento, 7-9 Febbraio 1996, 146-147.
- Chassefiere B. & Monaco A., 1987 - *Geotechnical properties and sedimentological processes of the Rhone continental margin*. *Marine Geology*, **74**, 225-235.
- Correggiari A., Roveri M. & Trincardi F., 1992 - *Regressioni forzate, regressioni deposizionali e fenomeni di instabilità in unità progradanti tardo quaternarie (Adriatico centrale)*. *Giorn. Geol.*, **54**, 19-36.
- Folk R.L. & Ward W.C., 1957 - *Brazos river: a study in the significance of grain size parameters*. *J. Sedim. Petrol.*, **27**(1), 3-26.
- Friedman G. M., 1961 - *Distinction between dune, beach, and river sands from their textural characteristics*. *J. Geol.*, **70**, 737-753, Chicago.
- Gensous B., Williamson D. & Tesson M., 1993 - *Late Quaternary transgressive and highstand deposits of a deltaic shelf (Rhône delta, France)*. *Spec. Publ. Int. Ass. Sediments*, **18**, 197-211.
- Got H., Aloisi J.C. & Monaco ??, 1985 - *Sedimentary processes in the Mediterranean deltas and shelves*. In: Stanley D.J., Wezer F.C. (eds.), *Geological evolution of the Mediterranean Basin*. Springer-Verlag, New York, 355-376.
- Jorissen F.J., Asioli A., Borsetti A.M., Capotondi L., De Visser J.P., Hilgen F.J., Rohling E.J., Van Der Borg K., Vergnaud Grazzini C. & Zachariasse W.J., 1993 - *Late Quaternary central Mediterranean bio-chronology*. *Mar. Micropaleont.*, **21**, 169-189.
- Müller C., 1979 - *Les Nannofossiles calcaires*. In: *Géologie Méditerranéenne*. Ed. de l'Université de Provence, 210-220
- Marani M., Taviani M., Trincardi F., Argnani A., & Borsetti A.M., 1986 - *Pleistocene Progradation and Postglacial Events of the Tyrrhenian continental shelf between the Tiber River Delta and Capo Circeo*. *Mem. Soc. Geol. It.*, **36**, 67-89, 11 ff.
- Pennetta M., 1996 - *Margine tirrenico orientale: morfologia e sedimentazione tardo pleistocenica-olocenica del sistema piattaforma scarpata continentale tra Capo Palinuro e Paola*. *Boll. Soc. Geol. It.*, **115**, 339-354.
- Pujol C. & Vergnaud Grazzini C., 1989 - *Paleoceanography of the Last Deglaciation in the Alboran Sea (Western Mediterranean)*. *Stable Isotopes and Planktonic Foraminiferal Records*. *Mar. Micropaleont.*, **15**, 153-179.
- Rio D., Raffi I. & Villa G., 1990 - *Pliocene Pleistocene calcareous nannofossil distribution patterns in the western Mediterranean*. In: Kastens K.A., Mascle J.

- et al.*, Proc. O.D.P. Sc. Res., **107**, 513-533.
- Rohling E.J., Jorissen F.J., Vergnaud Grazzini C. & Zachariasse W.J., 1993 - *Northern Levantine and Adriatic Quaternary planktic foraminifera; Reconstruction of paleoenvironmental gradients*. Mar. Micropaleont., **21**, 191-218.
- Rosignol-Strick M. & Planchais N., 1989 - *Climate patterns revealed by pollen and oxygen isotope records of a Tyrrhenian sea core*. Nature, **342**, 413-416.
- Shepard F.P., 1954 - *Nomenclature based on sand-silt-clay ratios*. J. Sedim. Petrol., **24**(3), 151-158.
- Snoeckx H. & Rea D.K., 1994 - *Dry bulk density and CaCO₃ relationships in upper Quaternary sediments of the eastern equatorial Pacific*. Marine Geology, **120**, 327-333.
- Trincardi F. & Normark W.R., 1988 - *Sediment waves on the Tiber prodelta slope: interaction of deltaic sedimentation and shelfal currents*. Geo-Mar. Lett., **8**, 149-157.
- Valia H. S. & Cameron B., 1977 - *Skewness as a paleoenvironmental indicator*. J. Sedim. Petrol., **47**(2), 784-793.

Ms received : May 22 , 1996
Sent to the A. for a revision: June 20, 1996
Final text received: Nov.10, 1996

Ms. ricevuto: 22 maggio 1996
Inviato all'A. per la revisione: 20 giugno 1996
Testo definitivo ricevuto: 10 novembre 1996